Paper No.
C2025-00177

AMPP ANNUAL CONFERENCE + EXPO
APRIL 6-10, 2025 | NASHVILLE, TENNESSEE

Analyzing Open Circuit Potential Change versus Time in Corrosion Inhibition Experiments: A Failed Attempt

Kushal Singla, Bruce Brown, Srdjan Nesic

Institute for Corrosion and Multiphase Technology (ICMT), Department of Chemical & Biomolecular Engineering, Ohio University, Athens, OH 45701

ABSTRACT

Use of organic corrosion inhibitors provides an economical and effective way for internal corrosion control of oil and gas production and transportation pipelines. The motivation to conduct corrosion inhibition measurements using electrochemical techniques was to get an indirect measurement of surface saturation concentration (SSC) for a model corrosion inhibitor compound, tetradecyldimethylbenzylammoniumbromide (BDA-C14), based on the steady state corrosion rate at different bulk inhibitor concentrations measured using a 2L glass cell setup. However, there was another important observation during corrosion inhibition experiments in the present study, which was a sudden rise in open circuit potential (OCP) to more positive values after injection of the corrosion inhibitor. In the present study, this OCP change is analyzed, and a detailed methodology is presented for the estimation of kinetic constants. Following some assumptions, OCP change vs. time data is used instead of the limited number of corrosion rate data points available in the transient region during inhibitor adsorption.

Keywords: Corrosion inhibitor, inhibitor adsorption, inhibition, open circuit potential

INTRODUCTION

For many years, our research group has been working to understand the adsorption of organic corrosion inhibitors using a range of experimental methods. Findings from one approach are cross-validated and supplemented by results from alternative experimental methods. Known model corrosion inhibitors, developed as part of the methodology for multiple researchers to study known surfactants, have been used in experiments

- to study the effect of corrosion inhibitors on electrochemical reactions,[1–5]
- to find out if there is a relationship between the critical micelle concentration and the concentration required to reach maximum corrosion mitigation,[6,7]
- to investigate the corrosion inhibitor adsorption structure on mica and mild steel at the nanoscale level using atomic force microscopy imaging of adsorbed molecular inhibitor layers,[8,9] and

- to quantify the adsorption kinetics and the nature of the adsorbed layer using a quartz crystal microbalance with dissipation monitoring (QCM-D).[10,11]

These different studies have shown agreement on multiple topics related to these corrosion inhibitors, except when focusing on the rate of inhibitor molecule adsorption versus the rate of corrosion mitigation. It seems there is a difference between the amount of time it takes for inhibitor molecules to adsorb on the metal surface and the amount of time it takes for the adsorbed inhibitor molecules to retard the active corrosion occurring on the metal surface.[10–13] This is assumed to be due to the difference in the methods used in collecting the data.

The research in this paper is focused on trying to determine if an electrochemical measurement from a potentiostat can give similar results to a mass-adsorption measurement given by a QCM-D in terms of the time taken to reach a steady state for corrosion inhibition experiments, and time taken to achieve adsorption/desorption equilibrium for QCM-D adsorption experiments. Experimental results of inhibitor adsorption experiments using QCM-D are reported in previous publications.[10,11] An observation made during corrosion inhibition experiments was that a sudden rise in open circuit potential (OCP) to more positive values occurred with the injection of corrosion inhibitor into the solution and this rise in potential has been linked to corrosion mitigation in previous studies.[2] This sudden change in OCP may help to link the two measurement methods.

This paper contains analysis of open circuit potential data recorded while conducting corrosion inhibition experiments reported in a previous publication.[12] The observation of a sudden rise in OCP occurred with injection of corrosion inhibitor, tetradecyldimethylbenzylammoniumbromide (BDA-C14), as shown in Figure 1. If this change in potential is understood to be directly related to the inhibitor adsorption step on the metal electrode, this result is consistent with the quartz crystal microbalance with dissipation monitoring (QCM-D) measurements reported by Singla, *et. al*, which also suggests that the adsorption step happens within minutes of inhibitor addition.[10,11]

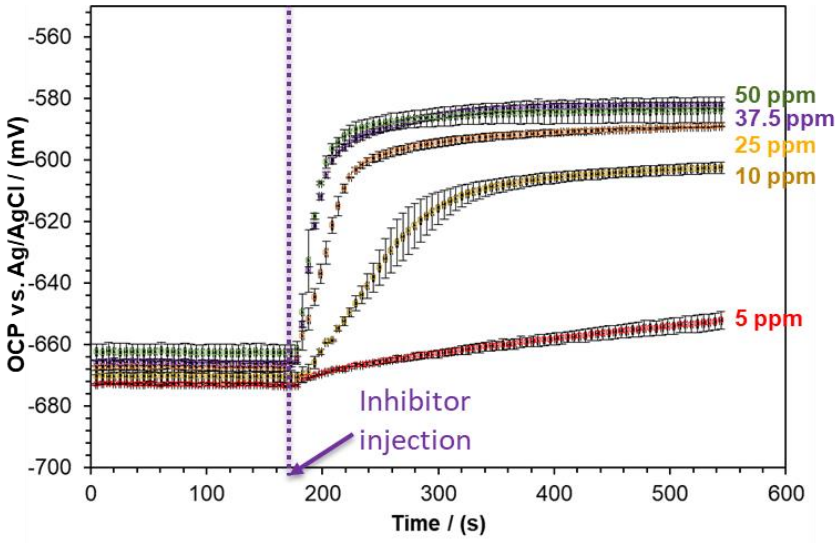

Figure 1: Open circuit potential measured with respect to time with inhibitor injection in solution phase. Experimental conditions: 1 wt. % aqueous NaCl solution, 1 bar CO_2, pH 4.00, and 30 °C.

EXPERIMENTAL PROCEDURE

For this study, the corrosion behavior of a quarternary ammonium type corrosion inhibitor, BDA-C14, is investigated. Corrosion experiments were conducted using a typical three-electrode, 2 L glass cell setup (Figure 2). An API 5L X65 rotating cylindrical electrode (RCE) was used as the working electrode with a rotating speed of 1000 rpm, a saturated Ag/AgCl electrode was used as the reference electrode, and a platinum covered titanium mesh was used as the counter electrode. For each experiment, the working electrode was polished with emery paper using 80, 120, 400 and 600 grit and then ultrasonically cleaned in isopropyl alcohol and dried with a nitrogen gas stream. More details on the experimental methodology is reported elsewhere.[12] Table 1 summarizes the experimental conditions.

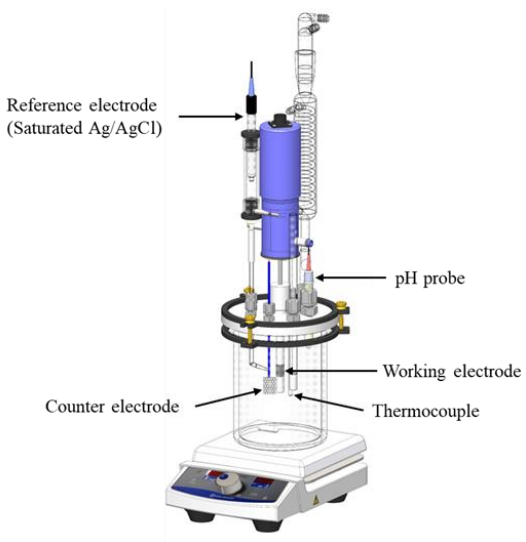

Figure 2: Schematic of the three-electrode glass cell setup. (Image courtesy: Cody Shafer)

Table 1: Test matrix for inhibitor adsorption studies

Parameter	Value
Working electrode, rotating cylindrical electrode (RCE)	API 5L X65
Reference electrode	saturated Ag/AgCl
Counter electrode	platinum covered titanium mesh
RCE rotational speed	1000 rpm
Sparge gas	CO_2
pH	4.00 ± 0.01
Temperature	30 ± 1 °C
Solution	1 wt. % NaCl in deionized water with different bulk inhibitor concentrations (5, 10, 25, 37.5 and 50 ppm(w))

RESULTS AND DISCUSSION

OCP change versus time for determination of kinetic constants

It has been reported previously in the inhibition model by Dominguez, et al., that the transient part of corrosion rate versus time can be used to extract kinetic adsorption/desorption constants.[1] However, it was observed that for the current set of corrosion inhibition experiments, the number of data points in the transient region are very small (2-3 points at one condition, please refer to the first figure in this previous publication).[12] Moreover, it was observed repeatedly that open circuit potential also changes with respect to time and stabilized to a value which seems to have a trend associated with bulk inhibitor concentration used (Figure 1). Since OCP was measured every 0.1 seconds and is a non-controlling, non-destructive electrochemical method, it would provide enough data in the first few minutes to analyze this change. Hence, the overall idea was to extract surface coverage versus time from OCP change versus time data and use this to estimate adsorption/desorption kinetic constants. But before getting into analyzing OCP change versus time data, it is first important to answer the question "why should the OCP of a corroding mild steel specimen change with the addition of an inhibitor?"

The change in OCP can be explained based on the change in reaction mechanism with addition of corrosion inhibitor. The explanation that an equal retardation of both anodic and cathodic reactions associated with mild steel corrosion under mass transfer control would result in a net positive change in corrosion potential was documented by Dominguez, et al (please refer to the first figure in this previous publication).[2] Clearly from Figure 3, when potentiodynamic sweeps are analyzed in conjunction with corrosion rate data, there is a shift of mechanism from limiting current control to activation control. The blank specimen corrosion rate was 4.2 mm/yr, $(i_{corr})_{\theta=0}$ = 4.2 A/m^2, while the final inhibited corrosion rate was 0.08 mm/yr, $(i_{corr})_{\theta=1}$ = 0.07 A/m^2 (Figure 3). The series of linear polarization resistance (LPR) measurements published previously[12] for 50 ppm(w) from 0 to 400 minutes are represented in Figure 3 by open diamond symbols showing their current density (i_{corr}) and potential measurements (E_{corr}) for each. It is important to notice here that, once the inhibitor had been added to the solution and the reaction was in activation control, the E_{corr} value did not change appreciably (−580mV to −620 mV), however, corrosion rates kept decreasing until steady state was reached. With this change of OCP with inhibitor injection (Figure 1), certain assumptions should be able to be made to mathematically convert the time dependent OCP change data to surface coverage versus time data for kinetic analysis. Assumptions are as follows:

i. Cathodic reaction remains in limiting current control for potential change data being analyzed.

ii. The slope of anodic reaction remains same. Geometric blockage principle.[14]

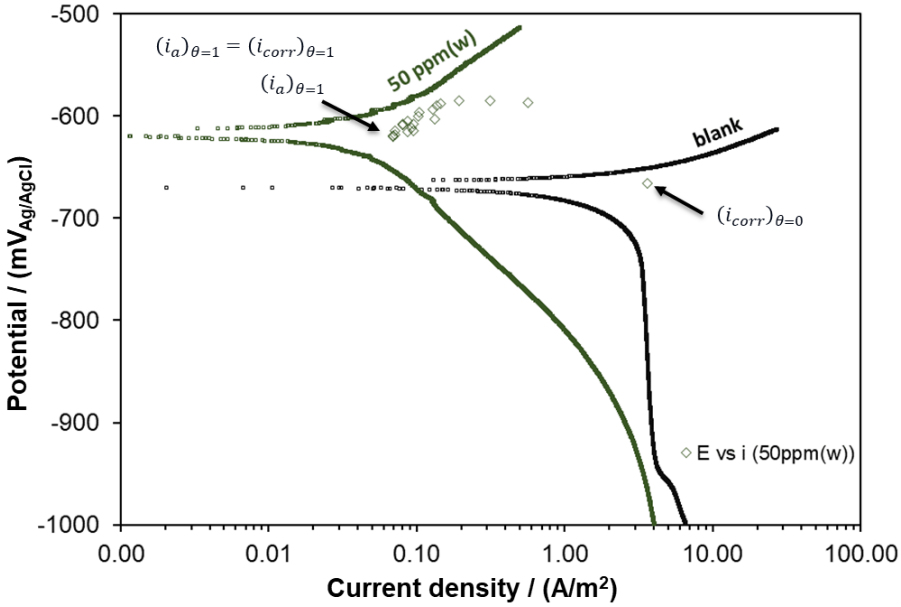

Figure 3: Potentiodynamic plots for two conditions blank (C_{inh} = 0ppm, black curves) and 50 ppm(w) (C_{inh} = 50ppm(w), green curves), for BDA-C14 model inhibitor compound at 30 °C, pH4.0, 100 rpm RCE and 0.96 bar CO_2. Also in this figure, corrosion rate measured for C_{inh} = 50 ppm(w) plotted against OCP; the first point representing blank solution corrosion rate measurement.

Methodology to track change in anodic reaction

Step 1: Since it was observed that OCP increases with inhibitor addition (Figure 1), and taking into account the assumptions mentioned above; corresponding to every point of potential change, a new anodic line can be drawn as shown in Figure 4.

Step 2: Now the retardation in anodic reaction can be tracked corresponding to OCP change assuming the overall reaction is in limiting current control. Hence, with this, surface coverage definition similar to Equation (1) can be used to convert OCP change *versus* time to surface coverage *versus* time at each inhibitor concentration tested.

$$\theta = \frac{(i_a)_{\theta=0} - (i_a)_{\theta}}{(i_a)_{\theta=0} - (i_a)_{\theta=1}} \quad (1)$$

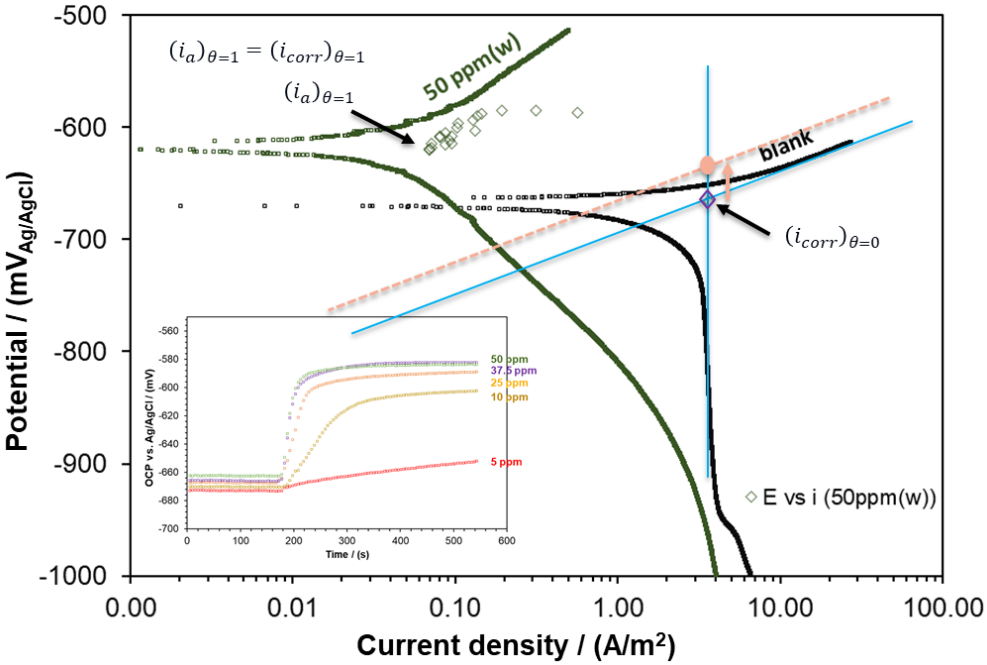

Figure 4: Schematic showing the methodology to draw a new anodic line at increased potential due to addition of corrosion inhibitor (dotted line). Picture in picture showing change in OCP vs. time with inhibitor injection for different bulk inhibitor concentrations.

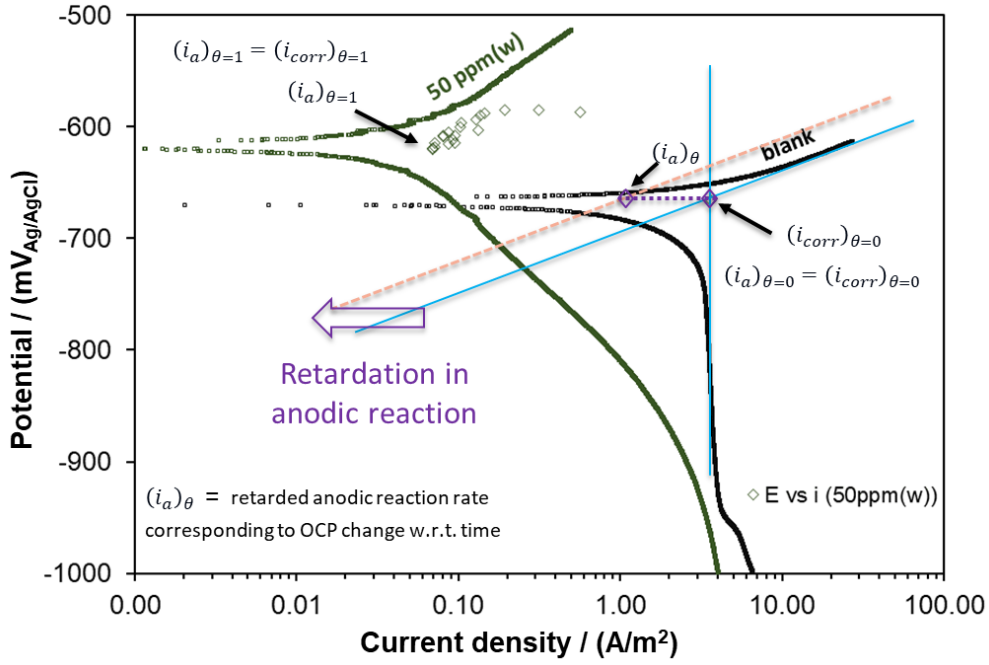

Figure 5: Schematic showing the methodology to track retardation in anodic reaction with increase in OCP with inhibitor injection.

Based on the methodology as described above and following the assumptions, surface coverage vs. time was calculated and is plotted in Figure 6.

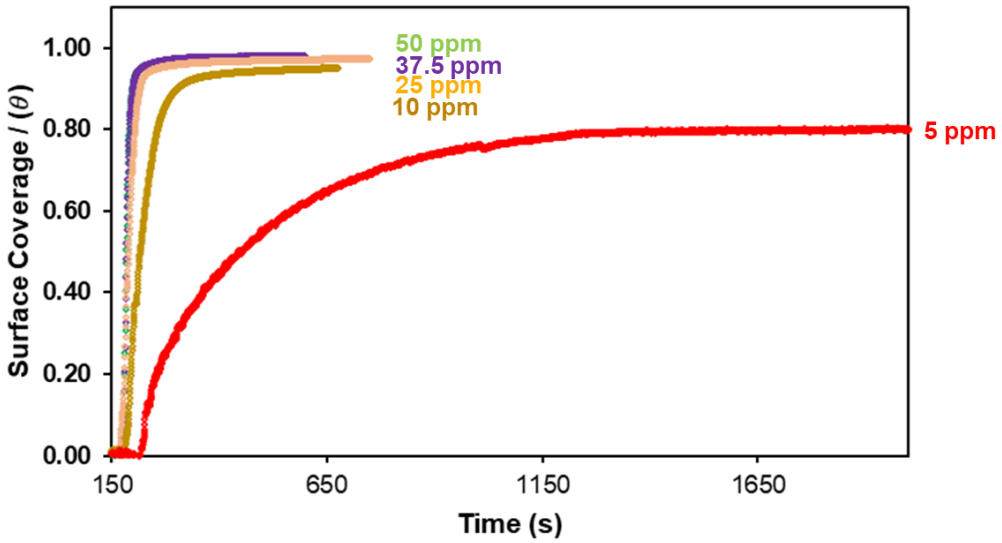

Figure 6: Surface coverage vs. time calculated from OCP change vs time.

Although, using the above methodology, surface coverage was calculated with respect to time using OCP change but, in reality, the underlying step was to convert potential to current density and then relate the change in current density to calculate surface coverage based on mentioned assumptions. So, as a checkpoint to assumptions stated above, surface coverage was also calculated from corrosion rate measurements (refer to Figure 1 in previous publication)[12] using Equation (2) and intersection point of these two alternate routes should provide us with a point on time scale up to with the assumptions stated above remains relevant.

$$\theta_{CR} = \frac{(CR)_0 - (CR)_i}{(CR)_0 - (CR)_{SSC}} \quad (2)$$

$(CR)_0$ - Steady state corrosion rate with no inhibitor (before inhibitor injection)

$(CR)_i$ - Inhibited steady state corrosion rate

$(CR)_{SSC}$ - Lowest corrosion rate achievable with a given inhibitor at given experimental conditions at surface saturation concentration (SSC)

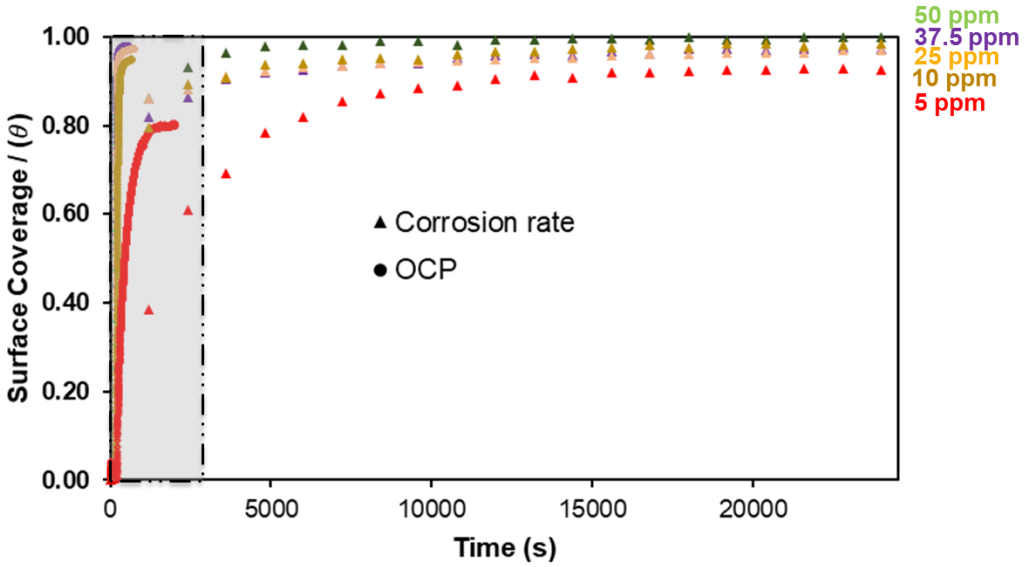

Figure 7: Surface coverage vs. time calculated from two different set of data (corrosion rate vs. time and OCP change vs. time).

The gray portion of Figure 7, zoomed in to the first 2500 seconds and analyzed for 50 ppm(w) bulk inhibitor concentration of BDA-C14, is shown in Figure 8. When looking at a particular data point at t=1200 seconds, there are two surface coverage values, one based on OCP change data and the other based on corrosion rate data. Clearly, there is a mismatch, and this mismatch was observed for all the tested concentrations and different time steps in measurements. This mismatch also signals the inherent flaw in this new approach to use OCP change for surface coverage calculations. Hence, as of now, based on this approach, it was impossible to identify the time range for which above mentioned assumptions would hold true and hence kinetic constants estimated using this methodology lacks fundamental support.

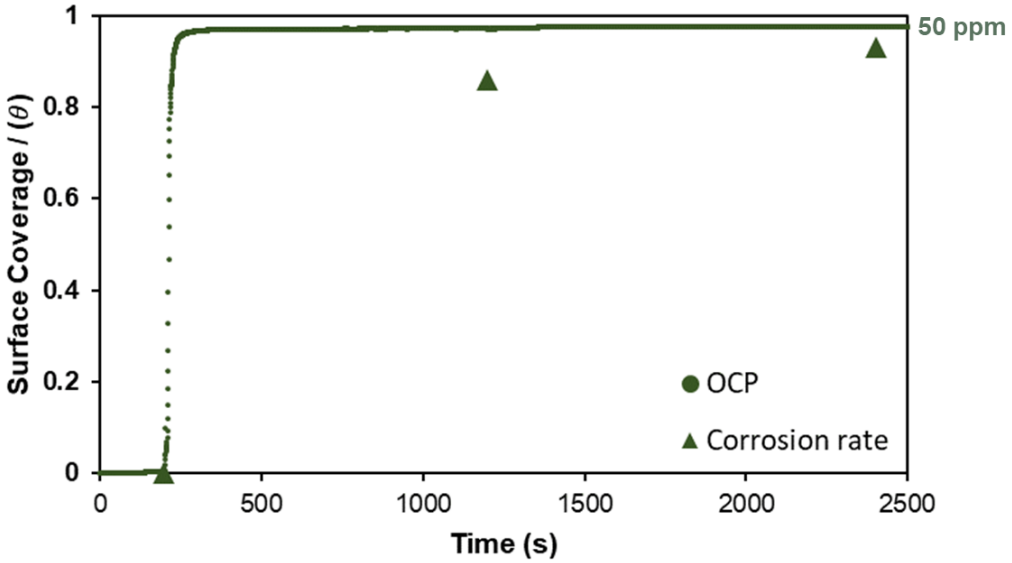

Figure 8: Zoomed in view of Figure 7 (gray area) showing surface coverage vs. time calculated from two different set of data for 50 ppm(w) bulk inhibitor concentration (corrosion rate vs. time and OCP change vs time).

SUMMARY

Inhibitor adsorption, as observed through QCM-D, reached equilibrium in approximately 15 minutes,[10,11] which aligns with the time required for OCP stabilization following inhibitor injection during electrochemical corrosion inhibition measurements. In contrast, the stabilization of corrosion rates measured *via*. LPR took about 120 minutes.[12] Notably even for the corrosion inhibition experiments, the most significant reduction in corrosion rate occurs within the first 15 minutes,[12] likely due to inhibitor adsorption resulting in inhibitor molecules replacing water molecules on the steel surface.

Hence, utilizing OCP change with respect to time was thought to be a possible solution for quantification of adsorption/desorption kinetics as compared to limited number of data points available in transient region for corrosion rate measurements. In this research, following certain assumptions, surface coverage was estimated with respect to time by tracking retardation in the anodic reaction using OCP change data. However, it was impossible to identify the time range for which those assumptions will hold true. Hence, to prove or disprove the validity of this analysis more supplementary data from independent measurements is needed.

ACKNOWLEDGEMENTS

The author would like to thank the following companies for their financial support:
Ansys, Baker Hughes, Chevron Energy Technology, Clariant Corporation, ConocoPhillips, ExxonMobil, M-I SWACO (Schlumberger), Multi-Chem (Halliburton), Occidental Oil Company, Pertamina, Saudi Aramco, Shell Global Solutions, and Total Energies.

REFERENCES

1. J.D. Olivo, Doctoral Dissertation, “Mechanistic Model of CO_2 Corrosion in the Presence of Organic Corrosion Inhibitors” (Athens, OH, 2019).

2. J.M. Domínguez Olivo, B. Brown, S. Nešić, “Modeling of Corrosion Mechanisms in the Presence of Quaternary Ammonium Chloride and Imidazoline Corrosion Inhibitors,” CORROSION 2016, paper no. 7406 (Houston, TX: NACE, 2016).

3. J.M. Domínguez Olivo, B. Brown, D. Young, S. Nešić, “Electrochemical Model of CO_2 Corrosion in the Presence of Quaternary Ammonium Corrosion Inhibitor Model Compounds,” CORROSION 2019, paper no. 13392 (Houston, TX: NACE, 2019).

4. J.D. Olivo, B. Brown, D. Young, S. Nešić, Corrosion 75 (2018): pp. 137-139, https://doi.org/10.5006/3076.

5. J.M. Domínguez Olivo, D. Young, B. Brown, and S. Nesic, “Effect of Corrosion Inhibitor Alkyl Tail Length on the Electrochemical Process Underlying CO_2 Corrosion of Mild Steel,” CORROSION 2018, paper No. 11537 (Houston, TX: NACE, 2018).

6. N. Moradighadi, S. Lewis, J.D. Olivo, D. Young, B. Brown, S. Nešić, Corrosion 77 (2021): pp. 266–275, https://doi.org/10.5006/3679.

7. Y. He, S. Ren, X. Wang, D. Young, M. Singer, Z. Belarbi, M. Mohamed-Saïd, S. Camperos, M.R. Khan, K. Cimatu, Corrosion 78 (2022): pp. 625–633, https://doi.org/10.5006/4086.

8. H. Wang, B. Brown, S. Nesic, and A. Pailleret, “Investigation of Inhibitor Adsorption Mechanism by in Situ Tapping Mode Atomic Force Microscopy,” CORROSION 2021, paper No.16610 (Houston, TX: AMPP, 2021).

9. H. Wang, S. Sharma, A. Pailleret, B. Brown, S. Nešić, Corrosion 78 (2022): pp. 990–1002, https://doi.org/10.5006/4136.

10. K. Singla, H. Perrot, B. Brown, and S. Nesic, “Adsorption of Model Inhibitor Compound Characterized Using Quartz Crystal Microbalance with Dissipation Monitoring,” CORROSION 2023, paper No. 19145 (Houston, TX: AMPP, 2023).

11. K. Singla, H. Perrot, B. Brown, and S. Nešić, *Corrosion* (2024): p. 4634, https://doi.org/10.5006/4634.

12. K. Singla, B. Brown, and S. Nešić, *Corrosion* 80 (2024): pp. 603–607, https://doi.org/10.5006/4514.

13. K. Singla, H. Perrot, O. Sel, B. Brown, and S. Nesic, “Use of Quartz Crystal Microbalance in Study of Inhibitor Adsorption,” CORROSION 2021, paper No. 16653 (Houston, TX: AMPP, 2021).

14. W.J. Lorenz, F. Mansfeld, *Electrochim Acta* 31 (1986): pp. 467–476.